Investigate the Effect of Chemical Post Processing on the Surface Roughness of Fused Deposition Modeling Printed Parts

Hind H. Abdulridha[1*], Tahseen F. Abbas[1], Aqeel S. Bedan[1]

[1] Production Engineering and Metallurgy Department, University of Technology-Iraq, Baghdad, Iraq
* Corresponding author's email: hind.h.abdulridha@uotechnology.edu.iq

ABSTRACT

Fused deposition modeling (FDM) technology is one of the rapidly growing techniques used for producing various complicated configurations without the need for any tools or continuous human intervention. However, a low quality of surfaces results for the layered production used in FDM. It is essential to investigate a suitable method for enhancing the accuracy and quality associated with FDM parts. This study aims to investigate the impact of different parameters such as the percentage of infill density, the shell thickness, layer thickness, and the number of top/bottom layers, as well as the percentage of infill overlap on part quality and the improvement of surface finish for printed specimens achieved through post-processing. Polylactic acid (PLA) material is used in building test specimens through the FDM approach. The experiments are carried out based on the Taguchi design of experiment method using (L25) orthogonal array. Using an analysis-of-variance approach (ANOVA), it is possible to understand the significance of the FDM parameters in order to find optimal parameter combinations. The results indicate that the application of the vapour smoothing procedure (VSP) treatment enhances the surface quality of FDM components to a microstage with minimal dimensional variation. The dichloromethane chemical has been found to exhibit excellent surface finish at an infill density of 50%, a layer thickness of 0.1 mm, a shell thickness of 2.8 mm, five top/bottom layer numbers, and 0.25 infill overlap.

Keywords: fused deposition modeling FDM, PLA, process parameters, ANOVA, chemical post-processing.

INTRODUCTION

Fused deposition modeling (FDM) stands out among additive manufacturing (AM) techniques, providing a means to construct 3D parts for both newly developed prototypes and challenging end-use components that conventional methods find difficult to produce [1, 2]. A 3D Computer-Aided Design model guides the selective layer-by-layer material combination for constructing the desired component [3]. In the FDM process, a hot filament is deposited layer by layer according to the computer-aided design (CAD) model. AM machines based on the filament extrusion principle are more commonly employed in industry than other AM principles, making FDM a popular additive manufacturing technology to fabricate plastic functional parts [4, 5]. The FDMs are capable of being built with Polylactic acid PLA, acrylonitrile butadiene styrene (ABS) thermoplastic, medical-grade ABS thermoplastic, and/or elastomer; however, PLA is currently the most popular material. In this current research work, PLA is used to fabricate parts using the FDM process. PLA is a commercially available material for printing samples. Polylactic acid (PLA) is extruded from nozzle tips as components or support materials onto an FDM machine-working platform [6, 7].

In comparison to other additive manufacturing methods, the staircase effect, a common issue in FDM parts, is caused by the layer-by-layer addition of materials, resulting in a poor surface finish that affects the performance of printed parts. This drawback, evident in dimensional inaccuracies, tends to overweigh the advantages of FDM parts [8, 9]. The quality of products created by

FDM is greatly influenced by a number of process parameters. It is believed that an optimal parameter set will improve the quality of 3D-printed objects and possibly save production time. The required FDM process parameters are typically determined by referencing the operator's skills and expertise or the operating manual [10]. Numerous studies have suggested statistical techniques to optimize the parameters for enhancing the FDM parts quality in terms of the desired response. Budzik et al. (2023) [11] presented the influence of specimen's internal structure printed in material extrusion (MEX) technique on the selected parameters. The FEA of the spline connection was performed by the procedure of unidirectional torsion of samples with various internal structures, and the results were compared with the test of unidirectional torsion of the connection. The results can serve as a basis for constructors designing parts with torsional strength that are produced utilizing MEX technology.

Chohan et al. (2022) [12] focused on optimizing hardness, surface finish, and dimensional accuracy in FDM and vapour smoothing processes. An algorithm of self-adaptive cuckoo search is used to predict the surface and dimensional features of functional prototypes and solve optimization issues. The results show a strong agreement between actual and predicted surface finish measurements. Kishorea et al. (2022) [13] aim to create a high-efficiency, low-cost system using chemicals to polish materials, specifically tetrahydrofuran (THF) and acetone. The system reduces the roughness of FDM specimens by over 95% with ideal input parameters. The system works best with minimal porosity and better-quality FDM specimens. The findings could help in developing a large-scale polishing system for FDM thermoplastic specimens and enhance their utilization in sectors that require highly polished parts.

Lavecchia et al. (2021) [14] proposed a quantitative analysis of ethyl acetate vapour chemical treatment for improving the surface finish of PLA-printed parts using 23 full parameter plans and roughness analysis to achieve a 90% reduction in roughness. The best results were achieved by increasing the solvent quantity duration of treatment while decreasing the low solvent quantity duration. The ethyl acetate vapour treatment was effective, allowing for the combination of FDM parameters with layer height and higher speed.

Budzik et al. (2021) [15] presented a methodology of quality control for AM parts printed form polymer materials, divided into models for visual presentation and manufacturing process needs. Data control, manufacturing control, and post-processing control are the three sections of the process. Several materials were used to create research models, with the PolyJet approach proving to be the most accurate. The authors suggest an AM's encompassing control system to satisfy Industry 4.0 needs. 3D printing methods, materials, and methods of measurement should consider both specificity and economic aspects.

Khosravani et al. (2021) [16] investigated the impact of post-processing on the mechanical characteristics of 3D-printed parts using Acrylonitrile Butadiene Styrene (ABS) material. Using the FDM method, test coupons were created, and a device was built for fixing imperfections. Fracture load and tensile strength were reduced upon surface treatment. The results can be used to optimize finishing processes and new designs.

Sugavaneswarn et al. (2021) [17] explored how FDM and vapour smoothing process parameters influence part quality by means of ANOVA with the TOPSIS method. The optimized multiple-criteria responses in terms of exposure time, build surface normal, and build orientation angle are recorded. The results indicate that VS is highly influential on up faces, having a minimal roughness of 0.11 μm and an error in one dimension measuring 0.01%. Dębski et al. (2021) [18] investigated the impact of 3D printing on the structure of machine elements made of polymeric materials after a torsion test. It was found that the type of polymer and the printing direction in FDM significantly influence the structure and torsional torque. The layered (FDM/FFF) has the highest dimensional and shape accuracy in the plane of applying layers but the lowest torsional strength due to the lowest torsional torque.

Li et al. (2021) [19] employed the Taguchi method to enhance the parts' surface finish by chemically treating them with chlorofom solution. The study shows temperature, concentration, and time govern surface roughness, but temperature holds the largest impact. The optimal parameter combinations are A2B4C4, and the results are consistent with the optimum solutions.

Prajapati and Rimza (2020) [20] explored the use of the vapour smoothing procedure (VSP) to enhance the surface quality of FDM components, focusing on the microstage with minimal dimensional variation. The study found improved floor quality in 1,2,-dichloroethane chemicals at specific conditions.

Panda et al. (2020) [21] investigated the impact of FDM parameters and post-processing treatment on the surface roughness of PLA objects produced by the FDM method. PLA is used as a biodegradable material in medical implants. Post-processing techniques include vapour smoothing, sanding, chemical treatment, and polishing. Taguchi design and Minitab software are used to optimize parameters. The dichloromethane chemical is found to be effective in dissolving PLA and reducing surface roughness.

Chohan et al. (2020) [22] used a chemical post-processing method utilizing acetone vapour with heated air. It examines the impact of orientation angle, finishing time, and finishing temperature using Taguchi, ANOVA, and TOPSIS multi-criteria optimization. The surface finish is highly responsive to temperature changes, with a 0° orientation angle yielding maximum strength. Higher temperatures aid in melting down FDM parts, and surface roughness increases with temperature. Anisotropic behaviour during tensile testing is also significant. The study found that surface finish is directly proportional to the time of finishing, as longer exposure leads to complete layer reflowing and settlement.

Singh et al. (2020) [23] developed a dedicated finishing apparatus for surface issues, using hot chemical vapours mixed with heated air for an excellent finish. Experiments showed higher temperatures and time-impaired surface finishes, but permanent weight gain in ABS parts could hinder usability. Several works have been presented to minimize surface roughness through FDM parameter optimization. The presence of layer lines on the surface of FDM parts makes post-processing very important. The surface roughness caused by the staircase effect is a result of these layer lines. An item with the best surface roughness increases its value and demand; thus, a product with a superior surface finish is in high demand these days. In the present work, an attempt has been made to optimize FDM parameters and post-processing treatments in order to improve the quality of FDM-printed specimens. First, ANOVA was used for optimizing the FDM parameters. Chemical vapour baths and chemical treatments were the two

post-processing procedures applied to the printed parts. In order to observe how pre-processing and post-processing treatments affected the surface quality of FDM parts, the macrostructures of the parts were recorded at each stage of printing.

EXPERIMENTAL WORK

Material and method

Lactic acid building blocks are used to create Polylactic (PLA), biodegradable, and bioactive polyester [7]. Because it can be produced at a low temperature and doesn't require a heated bed, it is the default filament used in the majority of extrusion-based 3D printers and is recommended in this work. PLA prints easily, is extremely inexpensive, and produces parts with a wide range of uses. In addition, it is one of the most renewable, biodegradable, and environmentally friendly filaments available today [24]. Furthermore, compared to ABS, 3D-printed PLA products have better mechanical characteristics [25]. But PLA has a drawback because it is brittle by nature [6]. Table 1 displays the characteristics and specifications of PLA filament.

Designing the component or part using a variety of design software is the first stage in the 3D printing process. The SOLIDWORKS 2022 program is used to prepare the computer-aided design (CAD) file. The 3D model needs to be transformed into a common format after being obtained, regardless of the method. STL is the most often used file type extension. This file format is widely used and works with a wide range of platforms and devices. The model then needs to be translated into the preferred 3D printing language. G-Code is the most widely used language, particularly for printers of the FDM type. This code instructs the target machine to travel in different directions and at varying speeds, modify the temperature of its components, activate its cooling components, and carry out a number of other tasks [27]. Figure 1 depicts the workflow for this work, which begins with the selection of FDM parameters and ends with performing

Table 1. PLA filament specifications and properties [26]

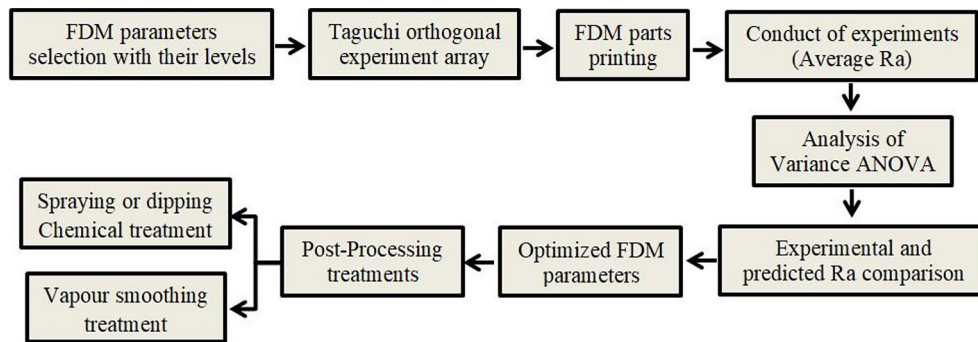| Property type	Melt point	Density at 21.5	Impact strength	Flexural strength	Tensile strength	Fracture elongation	Modulus of tensile
The value	195–235°C	1.25 g/cm^3	12 kJ/m	48–110 MPa	61–66 MPa	0.7%	2.7–16 GPa

Fig. 1. The proposed work flow

post-processing treatment to minimize the Ra value. Ultimaker Cura 4.13.1 software is used for advanced slicing. The CAD model and the sliced model for the specimen's average roughness Ra are shown in Figure 2a and b.

The design of the experiment influences the most critical levels and examines the behaviour of two or more components. The current investigation examines the effects of five different levels of each parameter on the quality of printed parts using FDM parameters, namely infill density%, shell thickness (mm), top / bottom layer number, layer thickness (mm), and infill overlap%. Based on expertise, actual industrial uses, and the equipment manufacturer's recommended acceptable minimum and maximum settings, the parameter

levels are chosen. Table 2 displays the process parameters used to print the parts, while Table 3 shows that other FDM parameters are maintained at their fixed levels.

It is necessary to use an appropriate optimization method in order to understand how the selected FDM process parameters affect the required output of the printed specimens. To find the optimum set of parameters, more samples must be prepared for testing at every possible combination of various processing parameters. This leads to the advantages of design of experiments (DOE), which minimizes the overall number of experiments, lowers manufacturing costs and times, and optimizes process parameters. A straightforward and practical method for
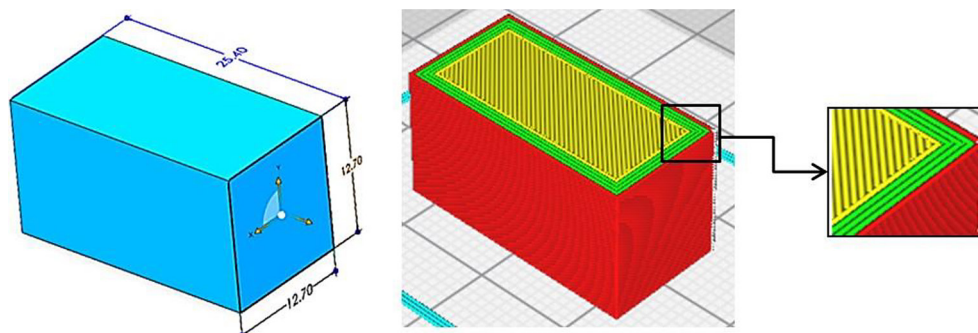

Fig. 2. CAD and sliced models for specimens

Table 2. Variable process parameters and their levels

Parameters	Levels				
	1	2	3	4	5
Infill density % (ID)	30	40	50	60	70
Layer thickness (LT) mm	0.1	0.15	0.2	0.25	0.3
Shell thickness (ST) mm	1.2	1.6	2	2.4	2.8
Top/bottom layer No. (TBL)	3	4	5	6	7
Infill overlap % (IO)	10	15	20	25	30

Table 3. Constant process parameters

Parameters	Value	Units
Printing speed	80	mm/sec
Infill pattern	Cubic	-
Printing temperature	200	°C
Build plate temperature	50	°C

optimizing processes and product design based on extensive experimental investigation is Taguchi DOE [28–30]. Many parameters can be optimized at the same time with fewer experiments, providing more quantitative results. Analyzing the impact of every parameter, measuring the optimum processing settings, and assessing the outcomes under ideal circumstances can be obtained by using the Taguchi technique. ANOVA, or the Signal-to-Noise S/N ratio, was utilized in the Taguchi approach to identify which performance characteristic diverges from the required values [26, 28]. The average surface roughness Ra of printed parts is minimized by data analysis using Minitab software based on the "smaller-the-better" SN ratio type. The S/N ratio for the smaller-the-better performance characteristic can be represented by Equation 1:

$$S/N = -10\,log(\tfrac{1}{n}\textstyle\sum_{i=1}^{n} y_i^2) \qquad (1)$$

where: n – total number of measurements, y_i – the characteristics value that was measured [26].

The Creality Ender-5 Pro machine is used to print specimens fabricated from TORWELL PLA material, as shown in Figure 3a with the printed specimens. The surface roughness (Ra) of each printed sample was measured using a profile measurement instrument (MarSurf PS1) with a 0.25 mm cut-off length, a 1.75 mm traversing length, and five sampling lengths, as indicated in Figure 3b. The average surface roughness (Ra) of the printed specimens was obtained by calculating the measurement three times perpendicular to the direction of the printed layers at different places on the same specimen.

RESULTS AND DISCUSSION

Surface roughness Ra results

The surface roughness Ra of 25 FDM specimens was measured after the printing process, as presented in Table 4 with its SN ratio. The results of the experiment are analyzed using Minitab 17. The best parameter level can be predicted using the S/N ratio main-effect plot. An analysis of the relative contributions of several parameters is done using a statistical ANOVA in order to identify which parameters significantly affect the performance characteristics as well as how they interact.

From Table 4, the surface roughness Ra was experimentally reduced from 10.71 to 5.22 μm in a specimen that was printed with 0.1 mm layer
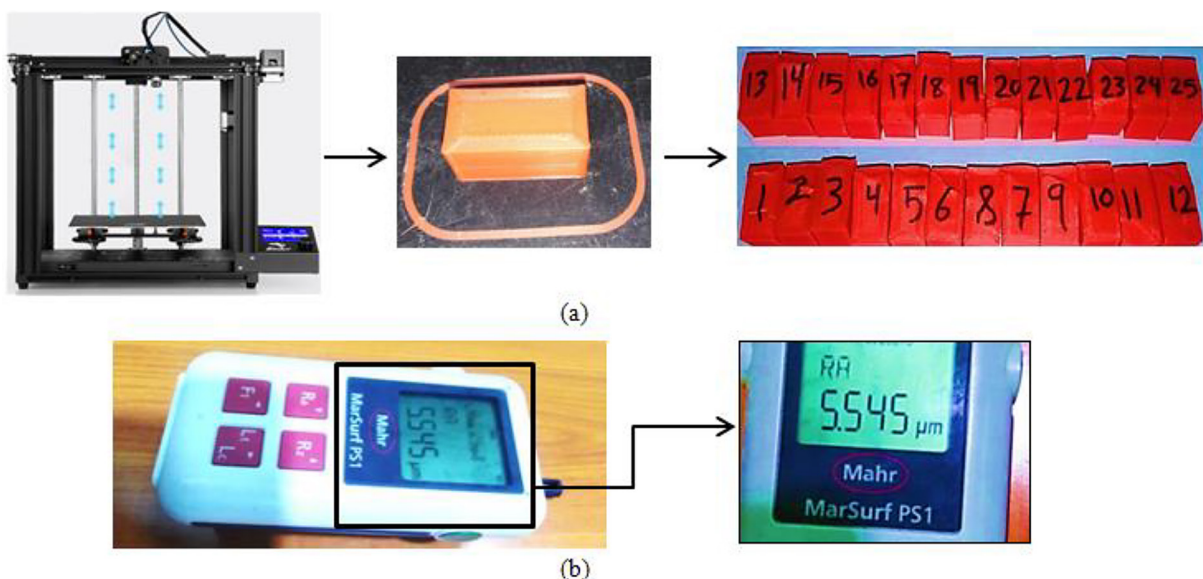

Fig. 3. (a) Test specimens printing process using Creality Ender-5 Pro 3D machine, (b) the surface roughness tester (MarSurf SP1)

Table 4. Experimental results for Ra and its signal-to-noise ratio

No.	Infill density %	Layer thickness (mm)	Shell thickness (mm)	Top/bottom layer no.	Infill overlap %	Average Ra (μm)	S/N ratio (dB)	Standard deviation of average Ra (μm)
1	30	0.10	1.2	3	10	6.31	-16.00	0.51
2	30	0.15	1.6	4	15	7.44	-17.43	0.16
3	30	0.20	2.0	5	20	9.20	-19.27	0.73
4	30	0.25	2.4	6	25	9.68	-19.72	0.01
5	30	0.30	2.8	7	30	8.80	-18.89	0.17
6	40	0.10	1.6	5	25	5.22	-14.35	0.08
7	40	0.15	2.0	6	30	8.33	-18.41	0.41
8	40	0.20	2.4	7	10	10.32	-20.27	0.39
9	40	0.25	2.8	3	15	8.90	-18.99	0.17
10	40	0.30	1.2	4	20	9.35	-19.42	0.32
11	50	0.10	2.0	7	15	6.70	-16.52	0.24
12	50	0.15	2.4	3	20	7.21	-17.15	0.08
13	50	0.20	2.8	4	25	8.19	-18.27	0.02
14	50	0.25	1.2	5	30	9.26	-19.33	0.27
15	50	0.30	1.6	6	10	9.63	-19.67	0.20
16	60	0.10	2.4	4	30	6.45	-16.19	0.50
17	60	0.15	2.8	5	10	6.66	-16.47	0.15
18	60	0.20	1.2	6	15	9.67	-19.70	0.15
19	60	0.25	1.6	7	20	8.77	-18.86	0.34
20	60	0.30	2.0	3	25	10.26	-20.23	0.66
21	70	0.10	2.8	6	20	6.80	-16.65	0.13
22	70	0.15	1.2	7	25	7.56	-17.57	0.37
23	70	0.20	1.6	3	30	9.50	-19.55	0.05
24	70	0.25	2.0	4	10	10.71	-20.60	0.55
25	70	0.30	2.4	5	15	9.61	-19.65	0.25

thickness, 5 top/bottom layer numbers, 40% infill density, 1.6 mm shell thickness, and 0.25 infill overlap. The results of the SN ratio indicate that the number 24 S/N ratio value represents the highest surface roughness, and the number 6 S/N ratio value gives the lowest roughness. When there is a negative signal-to-noise ratio, the signal needs to be amplified to make the value more important and positive. The SN ratio for surface roughness Ra has an arithmetic mean of -18.37 dB. Figure 4a and b shows the main effect graph of means and SN ratio for Ra, which shows how the layer thickness influences the surface roughness Ra of the FDM specimens significantly because it directly impacts the resolution and precision of the printed object. The surface roughness Ra of the specimen increased proportionally with increasing layer thickness. Thinner layers lead to finer details and smoother surfaces, thus enhancing overall dimensional accuracy.

To determine the printing parameter that has the greatest influence on surface roughness Ra, as well as to evaluate the P-value, Analysis of Variance (ANOVA) was utilized. Table 5 presents the percentage contribution of each parameter, individual P-values, F-values, and an R^2 of 95.16% for the surface roughness Ra data that were obtained. This suggests that the quadratic model that was predicted is suitable for providing a complete fit to the data. The linear parameters *LT*, the square, and the interaction parameters are statistically significant with a P value less than 0.05, according to the ANOVA Table's P-values. With a P-value of 0.003 at a 95% confidence level, it can be concluded that linear parameter (layer thickness) is the most important parameter influencing surface roughness Ra. Samples are prepared to undergo chemical treatment in order to validate our experiment after the optimum parameter value is determined and utilized again.

The influence of each FDM parameter at various levels can be identified because of the orthogonal experimental design. For instance, the surface roughness Ra mean for the infill density percentage at levels 1, 2, 3, 4, and 5 can be obtained by averaging the surface roughness Ra values from Table 4 for experiments 1 to 5, 6 to 10, 11 to 15, 16 to 20, and 21 to 25, respectively. A similar method can be used to calculate the Ra mean for each level of the other FDM parameters, as described in Table 6. Furthermore, the Ra total mean for all of the 25 experiments is computed and presented, which is represented by the dashed line in Figure 4b. After analyzing the results from Table 6 and Figure 4, it was considered that the optimal combination of FDM process parameters and their levels were as follows: the infill density at level 3, the layer thickness at level 1, the shell thickness at level 5, the number of top/bottom layers at level
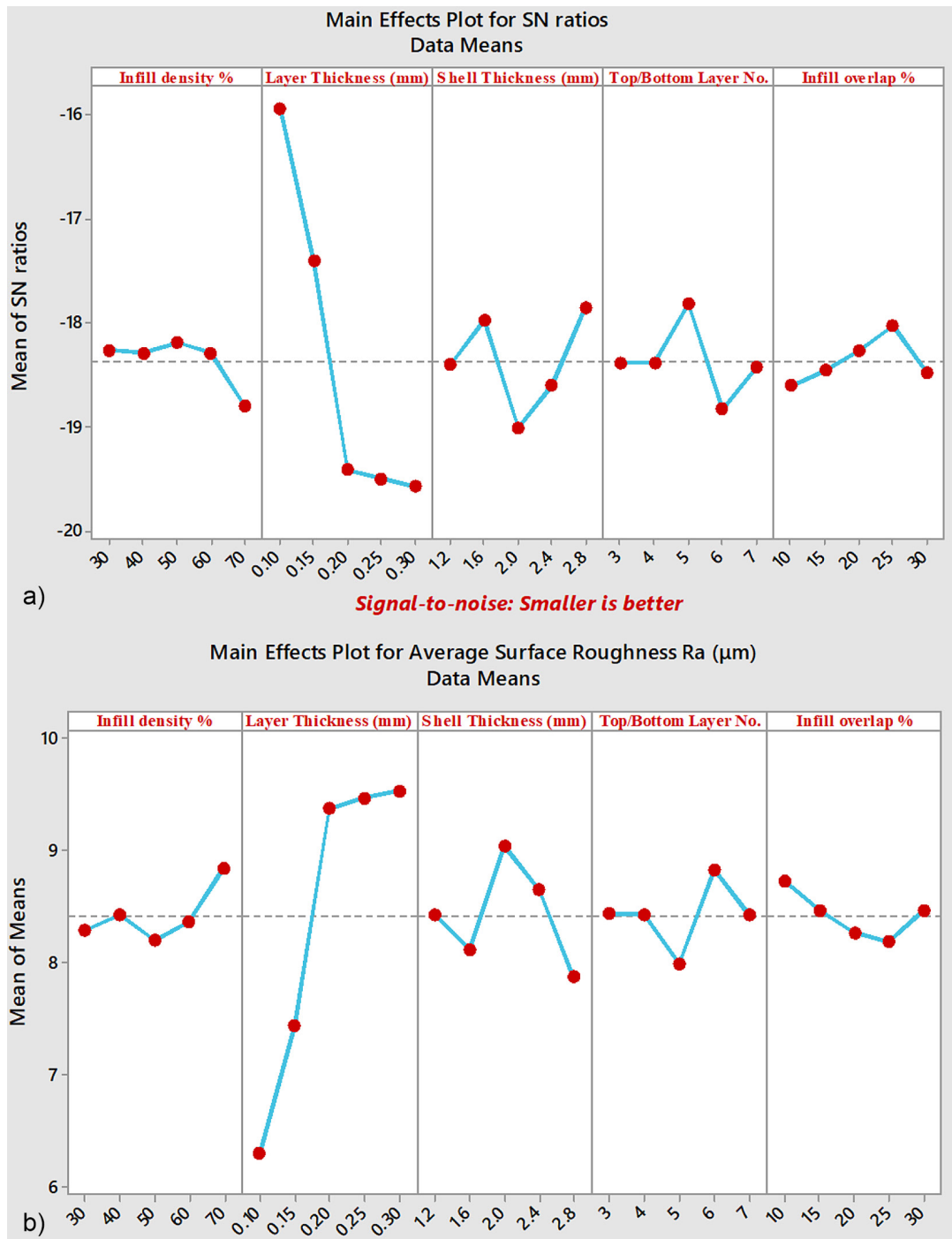

Fig. 4. (a) Main effect graph SN for Ra, (b) main effect graph mean for Ra

Table 5. ANOVA for surface roughness Ra (µm)

Source	DF	Adj SS	Adj MS	F-Value	P-Value
ID	1	0.4326	0.43257	1.19	0.311
LT	1	7.0688	7.06882	19.45	0.003
ST	1	0.2111	0.21107	0.58	0.471
TBL	1	0.1163	0.11634	0.32	0.589
IO	1	0.6144	0.61437	1.69	0.235
ID^2	1	0.6395	0.63952	1.76	0.226
LT^2	1	5.6558	5.65580	15.56	0.006
ST^2	1	0.0079	0.00788	0.02	0.887
TBL^2	1	0.1650	0.16500	0.45	0.522
IO^2	1	0.3892	0.38917	1.07	0.335
ID·LT	1	0.0202	0.02025	0.06	0.820
ID·ST	1	0.5799	0.57990	1.60	0.247
ID·TBL	1	0.4829	0.48293	1.33	0.287
ID·IO	1	0.1345	0.13452	0.37	0.562
LT·TBL	1	2.6349	2.63493	7.25	0.031
LT·IO	1	0.1961	0.19610	0.54	0.487
ST·IO	1	1.5131	1.51312	4.16	0.081
Error	7	2.5443	0.36347		
Total	24	52.5709			

Table 6. Ra mean for each level of FDM parameters

FDM parameters	Mean Ra				
	1	2	3	4	5
Infill density %	8.2868	8.423	8.196	8.3612	8.8342
Layer thickness (mm)	6.2952	7.4394	9.3736	9.463	9.53
Shell thickness (mm)	8.4292	8.1094	9.0396	8.6526	7.8704
Top/bottom layer no.	8.4354	8.4282	7.989	8.8202	8.4284
Infill overlap %	8.7256	8.4614	8.2632	8.184	8.467
Total mean Ra = 8.42024					

Table 7. Optimum level, significant and interactions of parameters from ANOVA

Parameters	Infill density %	Layer thickness (mm)	Shell thickness (mm)	Top/bottom Layer No.	Infill overlap %	Significant
Values	50	0.1	2.8	5	25	Layer thickness

3, and the infill overlap at level 4. Table 7 displays the optimal parameter level with significant parameters and interactions.

A predicted mathematical model was formulated based on the experimental results listed in Table 4, using Minitab 17 and employing regression analysis. This process involved fitting a model to the experimental data to establish a functional relationship between FDM parameters and response properties. Equation 2 represents the mathematical model for the relationship between FDM parameters and Ra. Considering various process parameters, they serve as a valuable tool for predicting Ra in our 3D printing process. The percentage error value between the predicted ANOVA results and measured surface roughness Ra of PLA specimens was calculated based on Equation 3, as shown in Figure 5, which presenting very small discrepancies. From Figure 5, the maximum and minimum percentage error between predicted and measured surface roughness Ra were 8.03% and 0.62%, respectively.
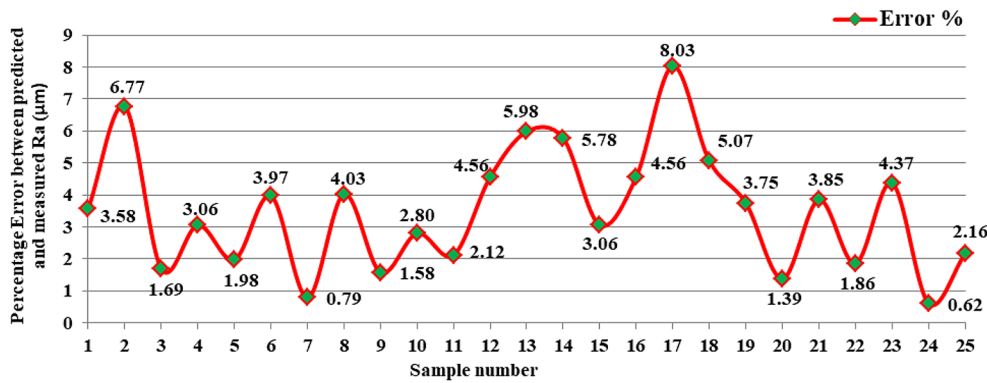
Fig. 5. The percentage error between experimental and predicted results of Ra in (µm)

$$Ra = 3.47 - 0.126(ID) + 119.8(LT) - 3.81(ST) + 0.86(TBL) - 0.372(IO) + 0.001058(ID)^2 - 174.9(LT)^2 - 0.145(ST)^2 + 0.106(TBL)^2 + 0.00459(IO)^2 - 0.050(ID \cdot LT) + 0.0469(ID \cdot ST) - 0.0171(ID \cdot TBL) + 0.00128(ID \cdot IO) - 4.60(LT \cdot TBL) - 0.331(LT \cdot IO) + 0.0871(ST \cdot IO) \quad (2)$$

$$Percentage\ Error = \left| \frac{Measured\ Ra - Predicted\ Ra}{Measured\ Ra} \right| \cdot 100 \quad (3)$$

Post-processing treatments

The surface roughness Ra of 25 specimens after printing using the FDM machine was measured by performing the Ra calculation three times perpendicular to the layer direction and then tacking the average value for each specimen as illustrated in Table 4. Without any post-processing treatment, the greater surface roughness value Ra of the specimen was 10.71 µm. This specimen will be subjected to a variety of treatments (chemical smoothing and vapour chemical smoothing) to determine whether the chemical treatment approach is capable of melting the layers in the printed specimens.

Chemical post-processing treatment

Chemical treatment is the quickest post-processing treatment method employed to enhance the surface quality of FDM-printed components [31, 32]. In this work, an organic compound such as acetone 99%, ethyl acetate 99.8%, and dichloromethane 99.5% with the properties illustrated in Table 8 will be selected based on the presented previous works to perform the required treatment. The chemical treatment can be applied to enhance the visual and physical properties of 3D-printed objects, providing a smoother and more refined finish, by putting the sample specimen on a plate

and treating it with the selected compounds using the spray method as shown in Figure 6a, while in the immersion method, an observation is made after the specimen is immersed in the chemical for 90 seconds, as shown in Figure 6b. The sample is left in the sun to dry after the procedure; the drying time may vary based on the type of chemical used, and then it is subjected to surface roughness and microstructure detection [23]. A popular chemical compound utilized in the post-processing of ABS material is acetone $(CH_3)_2CO$. It is used here to check if it is compatible with PLA. Whereas, ethyl acetate $C_4H_8O_2$ has gained popularity due to its low toxicity, ease of availability, affordability, speed of the procedure, and extremely low solvent concentration required. On the other hand, dichloromethane CH_2Cl_2 is a helpful solvent for many chemical processes because of its volatility and capacity to dissolve an extensive number of organic molecules. DCM is often known as methylene dichloride or methylene chloride. It is proposed in this work to find the chemical's dissolving potential because of its dissolving tendency [21, 22, 15]. The post-processing treatment with chemical treatment of the three compounds is shown in Table 9.

Vapour smoothing treatment

Using the chemical substances in vapour form, the vapour treatment method is utilized to smooth surface roughness. The same chemical that was utilized in the experiment was employed again with a vapour smoothing approach in the present study to measure the change in surface roughness after the chemical treatment was completed. Compared to other chemicals, dichloromethane is employed in the treatment because it significantly reduces the layer lines in chemical treatment from

Table 8. Properties of acetone, ethyl acetate, and dichloromethane

Properties	Acetone	Ethyl acetate	Dichloromethane
Molecular formula	$(CH_3)_2CO$, C_3H_6O	$C_4H_8O_2$	CH_2Cl_2
Density	0.7925 g/cc	902 kg/m³	1.3266 g/cm³
Mass of Molar	58.08 g/mol	88.11 g/mol	84.93 g/mol
Point of boiling	56.53 °C	77 °C	39.6 °C
Appearance	Colour less liquid	Colour less liquid	Colour less liquid
Point of melting	-94.9 °C	-83.6 °C	-96.7 °C

10.71 μm to 3.78 μm and 0.27μm using spraying and immersing, respectively. In the vapour smoothing approach, the chemical is heated up to 50 °C using a hot plate machine, as shown in Figure 6c. Since this chemical has a boiling point of 39.6 °C, dichloromethane begins to boil at this temperature, and the treatment is then completed utilizing the chemical's vapours. The specimen is exposed to the vapour for approximately fifteen minutes, and the result is recorded. Table 9 illustrates how the surface roughness tester measures the change in surface roughness.

Optimum specimen post-processing

The surface roughness of the specimen printed using the optimum parameter values obtained from the Taguchi design of the experiment was measured with a value equal to 6.83μm. Subsequently, the samples undergo post-processing techniques to determine the amount of surface roughness reduction. Using optimum values for vapour chemical smoothing, it can be observed from the microstructure of different experiments that layer lines gradually disappear from the raw sample. The layer lines are obvious in the specimen in which post-processing is not applied. However, the layer lines dissolve after the chemical treatment.

When compared to other chemicals, dichloromethane provides the best results as it is able to dissolve PLA material. Utilizing the Taguchi design of experimentation, the most important parameter is optimized to produce a result of 6.83 μm after optimization. Furthermore, the surface roughness Ra value decreased to 0.18 μm, which is extremely small, by performing the vapour chemical treatment on the optimal specimen. Surface roughness Ra values are displayed in Table 9, along with various post-processing results.

Surface topography is crucial for understanding the quality of the printed surface. Therefore, critical experimental observations were conducted using a Stereo microscope, and these results are presented in Figure 7. As depicted in Figure 7a, specimens formed with 70% density, 0.25 mm thickness of layer, shell thickness of 2 mm, 4 top/bottom layer numbers, and infill overlap of 0.1 exhibit rough surfaces equal to 10.71 μm. In contrast, Figure 7b-d illustrates specimens that were subjected to spray chemical treatment with acetone, ethyl acetate, and dichloromethane, respectively, where the minimum roughness obtained was equal to 3.78 μm by processing the specimen with dichloromethane. Figure 7e-g illustrates specimens that were subjected to immersion with chemical treatment through acetone,

Table 9. Surface roughness and identification of microstructure in prepared samples

| No.	Post-processing techniques	Method	Average surface roughness Ra (μm)	Deviation %
1	Ra before post-processing technique	Directly printed FDM part	10.71	0.81
2	Chemical treatment	Acetone	Spraying = 6.52 Immersing = 4.88	0.04 0.74
3	Chemical treatment	Ethyl acetate	Spraying = 7.15 Immersing = 6.05	0.5 0.16
4	Chemical treatment	Dichloromethane	Spraying = 3.78 Immersing = 0.27	0.77 0.37
5	Optimized specimen	Orthogonal array, S/N ratio, Minitab software	6.83	0.62
6	Vapour smoothing for an optimized specimen	Dichloromethane	0.18	0.56

(a)

(b)

(c)
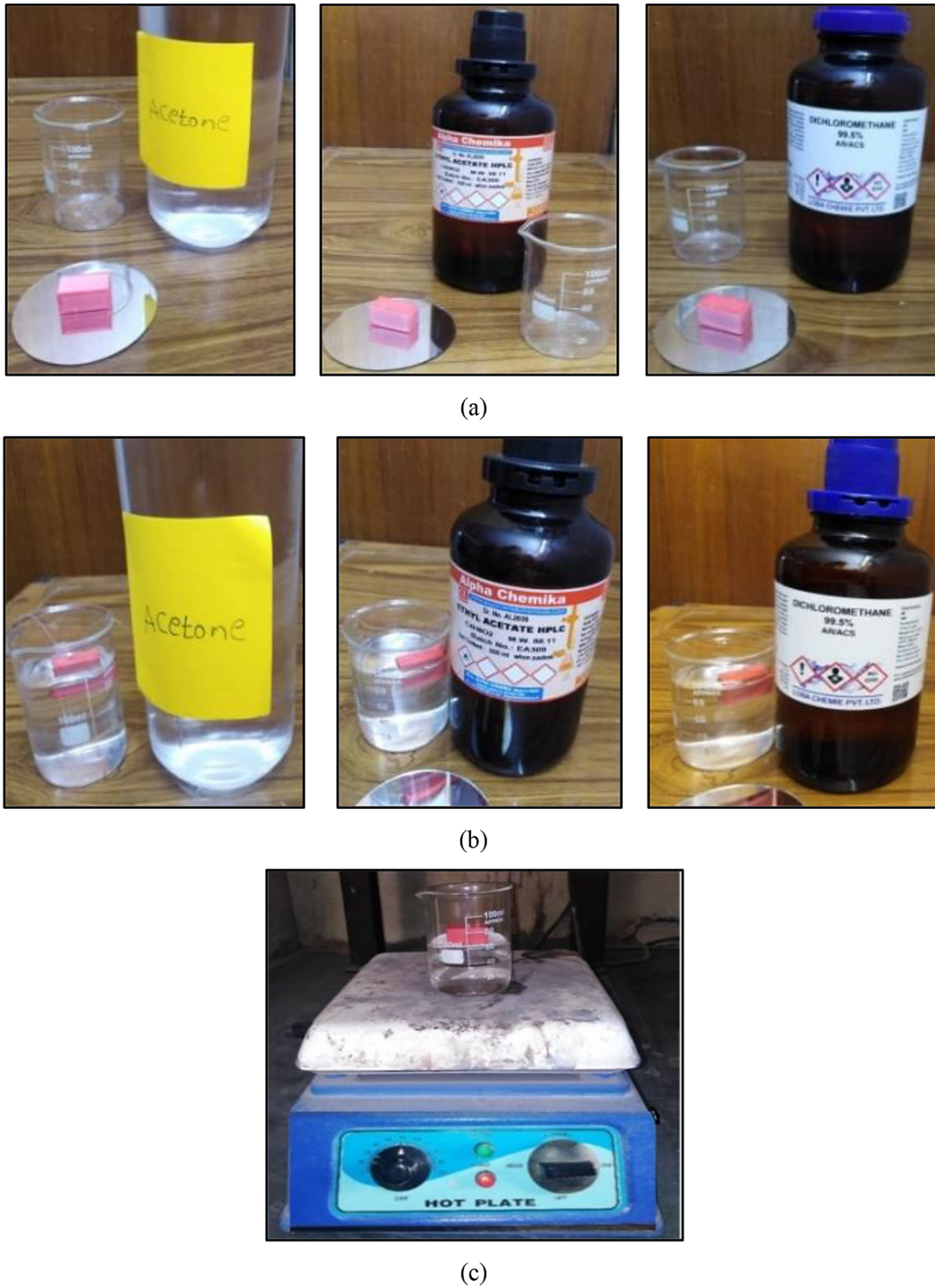
Fig. 6. Chemical post-processing approach by (a) spraying, (b) immersing, of acetone, ethyl acetate, and dichloromethane, (c) vapour chemical post-processing technique

ethyl acetate, and dichloromethane, respectively, which reduced the roughness of the printed specimen to 0.27 μm using dichloromethane. Figure 7h illustrates a specimen that was subjected to vapour chemical treatment through dichloromethane, which reduced the roughness of the printed specimen to 0.18 μm. The reduction in the roughness of PLA-printed samples when using dichloromethane is likely due to its solvent action and smoothing capabilities. Dichloromethane can interact with the outer layers of PLA, causing them to become more malleable or slightly dissolve. The material can be redistributed, filling in gaps and irregularities created by the layer-by-layer FDM printing process and creating a more homogeneous and aesthetically pleasing surface.
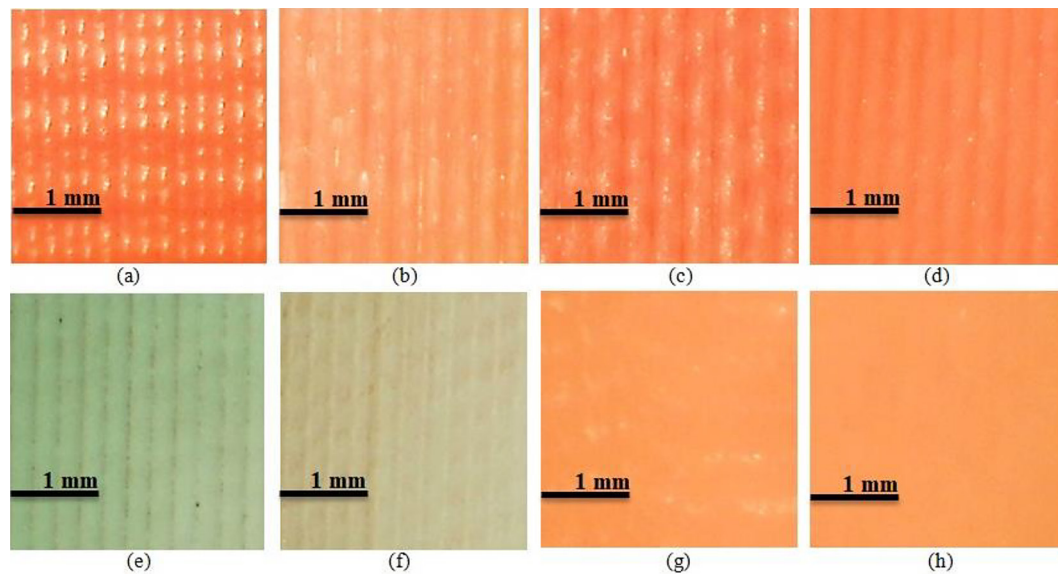
Fig. 7. Surface topography of the printed samples using a stereo microscope at 20x magnification before and after post-processing techniques for (a) maximum Ra value before post-processing, (b) spraying with acetone (c) spraying with ethyl acetate, (d) spraying with dichloromethane, (e) immersing with acetone, (f) immersing with ethyl acetate, (g) immersing with dichloromethane, and (h) vapour smoothing by dichloromethane

While vapour treatment can reduce the surface roughness Ra of the PLA specimens, it's crucial to recognize the limitations in the results and analysis, particularly its impact on dimensional accuracy, as illustrated in Table 9, where the average percentage deviation reaches 0.56% through vapour smoothing using dichloromethane. Additionally, the utilization of solvents in vapour smoothing, such as dichloromethane or acetone, poses health hazards. Therefore, it is important to implement thorough safety precautions, including the utilization of proper ventilation and personal protective equipment, to minimize related risks.

CONCLUSIONS

Imprecise dimensional accuracy and poor surface finish are two issues with FDM products. These problems can be effectively solved by optimizing the machine's parameters and treating the FDM parts with post-processing techniques. To reduce surface roughness, FDM parameters have been optimized utilizing Taguchi's method. PLA objects that were printed according to the optimized process parameter will be subjected to chemical vapour treatment with dichloromethane as a post-processing procedure. The following conclusions could be drawn. Experimental results revealed that the highest average roughness (Ra) of 10.71μm was achieved at 70% infill density,

2 mm shell thickness, 0.25 mm layer thickness, four top/bottom layers, and 0.1 infill overlap. Analysis of variance (ANOVA) results emphasized that layer thickness is the primary parameter influencing surface roughness. A lower surface roughness Ra of 6.83 μm was achieved in the PLA object created by optimizing a process parameter. It was found that dichloromethane was effectively employed for removing layer lines, which are typically presented in the parts printed by the FDM process. It may significantly reduce the surface roughness of extremely complicated items. Chemical treatment using dichloromethane reduced surface roughness Ra from 10.71 μm to 0.27 μm, which was the lowest of all chemical post-processing treatments. However, material loss and weight increases occurred in order to achieve the surface enhancement. Moreover, the chemical type and its concentration were found to have a significant impact on the surface quality of FDM parts. Chemical vapour treatment with dichloromethane produced a glossy and attractive PLA surface with a roughness of 0.18μm. This was achieved at 50% infill density, 0.1 mm layer thickness, 2.8 mm shell thickness, five top/bottom layers, and 0.25 infill overlap, without material loss or an increase in the weight of the FDM parts. In the current investigation, vapour chemical treatment proved to be the most effective post-processing treatment when taking into account the surface roughness values obtained.

REFERENCES

1. Fafenrot S., Grimmelsmann N., Wortmann M., Ehrmann A. Three-dimensional (3D) printing of polymer-metal hybrid materials by fused deposition modeling. Materials 2017; 10(10): 1199. https://doi.org/10.3390/ma10101199

2. Ahmad S.M., Ezdeen S.Y. Effect of coating on the specific properties and damping loss parameter of ultem 1010. ZANCO Journal of Pure and Applied Sciences 2021; 33(2): 105–116. http://dx.doi.org/10.21271/zjpas

3. Abbas T., Othman F.M., Ali H.B. Effect of infill parameter on compression property in FDM process. International Journal of Engineering Research and Application 2017; 7(10): 16–19. https://doi.org/10.9790/9622-0710021619

4. Gibson I., Rosen D., Stucker B., Khorasani A. Additive manufacturing technologies – 3D printing, rapid prototyping, and direct digital manufacturing. Springer, Business Media, New York, NY, 2015. https://doi.org/10.1007/978-1-4939-2113-3

5. Vyavahare S., Teraiya S., Panghal D., Kumar S. Fused deposition modelling: a review. Rapid Prototyping Journal 2020; 26(1): 176–201. https://doi.org/10.1108/rpj-04-2019-0106

6. Naser F.A., Rashid M.T. The Influence of Concave Pectoral Fin Morphology in the Performance of Labriform Swimming Robot. Iraqi Journal for Electrical and Electronic Engineering 2020; 16(1): 54–61. https://doi.org/ 10.37917/ijeee.16.1.7

7. Aldeen N.A., Sadkhan B.A., Owaid B. Hand bone orthosis manufacturing using 3d printing technology. Journal of Engineering and Sustainable Development 2020; 24(Special): 451–458. https://doi.org/10.31272/jeasd.conf.1.50

8. Kruth J.P., Levy G., Klocke F., Child T.H.C. Consolidation phenomena in laser and powder-bed based layered manufacturing. CIRP Annals – Manufacturing Technology 2007; 56(2): 730–759. https://doi.org/ 10.1016/j.cirp.2007.10.004

9. Gebhardt A. Understanding additive manufacturing. Carl Hanser Verlag, Munich, 2012.

10. Sood A.K., Ohdar R.K., Mahapatra S.S. Improving dimensional accuracy of fused deposition modeling processed part using grey Taguchi method. Materials & Design 2009; 30(10): 4243–4252. https://doi.org/10.1016/j.matdes.2009.04.030

11. Budzik G., Dziubek T., Przeszłowski Ł.P., Sobolewski B., Dębski M., Gontarz M.E. Study of unidirectional torsion of samples with different internal structures manufactured in the MEX process. Rapid Prototyping Journal 2023; 29(8): 1604–1619. https://doi.org/10.1108/RPJ-09-2022-0332

12. Chohan J.S., Mittal N., Singh R., Singh U., Salgotra R., Kumar R., Singh S. Predictive modeling of surface and dimensional features of vapour-smoothened FDM parts using self-adaptive cuckoo search algorithm. Progress in Additive Manufacturing 2022; 7: 1023–1036. https://doi.org/10.1007/s40964-022-00277-8

13. Kishore S.R., Mathew A., Tomy A.T., Sugavaneswaran M., Rajan A.J. Design and development of hot vapour polishing system and optimization of it's process parameters for FDM printed parts. Tribology in Industry 2022; 44(4): 551–567. https://doi.org/10.24874/ti.1305.05.22.09

14. Lavecchia F., Guerra M.G., Galantucci L.M. Chemical vapor treatment to improve surface finish of 3D printed polylactic acid (PLA) parts realized by fused filament fabrication. Progress in Additive Manufacturing 2022; 7: 65–75. https://doi.org/10.1007/s40964-021-00213-2

15. Budzik G., Woźniak J., Paszkiewicz A., Przeszłowski Ł., Dziubek T., Dębski M. Methodology for the Quality Control Process of Additive Manufacturing Products Made of Polymer Materials. Materials 2021; 14(9): 2202. https://doi.org/10.3390/ma14092202

16. Khosravani M.R., Schüürmann J., Berto F., Reinicke T. On the post-processing of 3D-printed ABS parts. Polymers 2021; 13(10): 1559. https://doi.org/10.3390/polym13101559

17. Sugavaneswarn M., Prashanthi B.A., John J.R. A multi-criteria decision making method for vapor smoothening fused deposition modelling part. Rapid Prototyping Journal 2021; 28(2): 236–252. https://doi.org/10.1108/rpj-08-2020-0184

18. Dębski M., Magniszewski M., Bernaczek J., Przeszłowski Ł., Gontarz M., Kiełbicki M. Influence of Torsion on the Structure of Machine Elements Made of Polymeric Materials by 3D Printing. Polimery 2021; 66(5): 298–04. https://doi.org/10.14314/polimery.2021.5.3

19. Li B., Yang J., Gu H., Jiang J., Zhang J., Sun J. Surface roughness of PLA parts by FDM with chemical treatment. Journal of Physics: Conference Series 2021; 1948: 012199. https://doi.org/10.1088/1742-6596/1948/1/012199

20. Prajapati M., Rimza S. An experimental study of surface improvement in FDM parts by vapor treatment process. Journal of Mechanical Engineering Research 2020; 3(1): 12–20. https://doi.org/10.30564/jmer.v3i1.1681

21. Panda S.S., Chabra R., Kapil S., Patel V. Chemical vapour treatment for enhancing the surface finish of PLA object produced by fused deposition method using the Taguchi optimization method. SN Applied Sciences 2020; 2(916). https://doi.org/10.1007/s42452-020-2740-1

22. Chohan J.S., Kumar R., Singh T.B., Singh S., Sharma S., Singh J., Mia M., Pimenov D. Y.,

Chattopadhyaya S., Dwivedi S.P., Kapłonek W. Taguchi S/N and TOPSIS based optimization of fused deposition modelling and vapor finishing process for manufacturing of ABS plastic parts. Materials. 2020; 13(22): 5176. https://doi.org/10.3390/ma13225176

23. Singh T.H.B., Chohan J.S., Kumar R. Performance analysis of vapour finishing apparatus for surface enhancement of FDM parts. Materials Today proceedings 2020; 26(5): 3497–3502. https://doi.org/10.1016/j.matpr.2020.04.553

24. Buys Y.F., Aznan A.N.A., Anuar H. Mechanical properties, morphology, and hydrolytic degradation behavior of polylactic acid/natural rubber blends. IOP Conference Series: Materials Science and Engineering 2018; 290(1): 12077. https://doi.org/10.1088/1757-899X/290/1/012077

25. Rismalia M., Hidajat S.C., Permana I.G.R., Hadisujoto B., Muslimin M., Triawan F. Infill pattern and density effects on the tensile properties of 3D printed PLA material. Journal of Physics: Conference Series 2019; 1402(4): 44041. https://doi.org/10.1088/1742-6596/1402/4/044041

26. Abdulridha H.H., Abbas T.F. Analysis and investigation the effect of the printing parameters on the mechanical and physical properties of PLA parts fabricated via FDM printing. Advances in Science and Technology Research Journal 2023; 17(6): 49–62. https://doi.org/10.12913/22998624/173562

27. Dey A., Yodo N. A systematic survey of FDM process parameter optimization and their influence on part characteristics. Journal of Manufacturing and Materials Processing 2019; 3(3): 64. https://doi.org/10.3390/jmmp3030064

28. Maguluri N., Suresh G., Rao K.V. Assessing the effect of FDM processing parameters on mechanical properties of PLA parts using Taguchi method, Journal of Thermoplastic Composite Materials 2021; 36(10): 1–17. https://doi.org/10.1177/08927057211053036

29. Noor H., Ibrahim M., Wahab M.S., Zahid M.S. Evaluation of FDM pattern with ABS and PLA material. Applied Mechanics and Materials 2014; 465–466: 55–59. https://doi.org/10.4028/www.scientific.net/AMM.465-466.55

30. Mohamed O.A., Masood S.H., Bhowmik J.L. Optimization of fused deposition modelling process parameters: a review of current research and future prospects. Advances in Manufacturing 2015; 3(1): 42–52. https://doi.org/10.1007/s40436-014-0097-7

31. Hambali R.H., Cheong K.M., Azizan N. Analysis of the influence of chemical treatment to the strength and surface roughness of FDM. IOP Conference Series Materials Science Engineering 2017; 210: 1–9. https://doi.org/10.1088/1757-899X/210/1/012063

32. Lalehpour A., Barari A. Post processing for fused deposition modeling parts with acetone vapour bath. IFAC-PapersOnLine 2016; 49(31): 42–48. https://doi.org/10.1016/j.ifacol.2016.12.159